

Coping with Junk Radiation in Binary Black Hole Simulations

Kenny Higginbotham,¹ Bhavesh Khamesra,¹ Jame P. McInerney,¹
Karan Jani,¹ Deirdre M. Shoemaker,¹ and Pablo Laguna¹

¹*Center for Relativistic Astrophysics, School of Physics,
Georgia Institute of Technology, Atlanta, GA 30332*

Spurious junk radiation in the initial data for binary black hole numerical simulations has been an issue of concern. The radiation affects the masses and spins of the black holes, modifying their orbital dynamics and thus potentially compromising the accuracy of templates used in gravitational wave analysis. Our study finds that junk radiation effects are localized to the vicinity of the black holes. Using insights from single black hole simulations, we obtain fitting formulas to estimate the changes from junk radiation on the mass and spin magnitude of the black holes in binary systems. We demonstrate how these fitting formulas could be used to adjust the initial masses and spin magnitudes of the black holes, so the resulting binary has the desired parameters after the junk radiation has left the computational domain. A comparison of waveforms from raw simulations with those from simulations that have been adjusted for junk radiation demonstrate that junk radiation could have an appreciable effect on the templates for LIGO sources with SNRs above 30.

PACS numbers: 04.25.D-, 04.25.dg, 04.30.Db, 04.80.Nn

Introduction: This letter presents a method to deal with the spurious *junk* radiation present in puncture-type initial data for binary black hole (BBH) simulations.

When Einstein's theory of General Relativity is viewed as an initial-value problem, the initial data consist of the spatial metric γ_{ij} and the extrinsic curvature K_{ij} of the initial space-like hypersurface in the space-time foliation. In the pair $\{\gamma_{ij}, K_{ij}\}$, not everything is freely specifiable. Four *pieces* are fixed by the Hamiltonian and momentum constraints. The York-Lichnerowicz approach [1, 2] provides a path to identify those four pieces via conformal transformations and tranverse-traceless decompositions. With this approach, after assuming conformal flatness ($\gamma_{ij} = \Phi^4 \eta_{ij}$) and vanishing trace of the extrinsic curvature ($K_i^i = 0$), the Hamiltonian constraint for vacuum space-times reads:

$$\tilde{\Delta}\Phi + \frac{1}{8}\Phi^{-7}\tilde{A}_{ij}\tilde{A}^{ij} = 0. \quad (1)$$

Here, tildes denote tensors and operators in conformal space, and \tilde{A}_{ij} is the conformal trace-free extrinsic curvature satisfying $\tilde{\nabla}_i\tilde{A}^{ij} = 0$, namely the momentum constraint.

To construct puncture-type initial data representing BBHs, one uses the Bowen-York [3] point-source solutions to $\tilde{\nabla}_i\tilde{A}^{ij} = 0$:

$$\tilde{A}^{ij} = \frac{3}{2r^2} [P^i l^j + P^j l^i - (\eta^{ij} - l^i l^j)(P^k l_k)] \quad (2)$$

$$\tilde{A}^{ij} = \frac{6}{r^3} l^{(i} \epsilon^{j)kl} S_k l_l \quad (3)$$

with $l^i = x^i/r$ and ϵ^{ijk} the Levi-Civita symbol. Also, P^i and S^i are the linear and angular momentum of the point-source, respectively. Given (2) and (3), Eq. (1) is solved using the *puncture* approach introduced by Brandt and Brügmann [4]. The essence of this approach is to

factor out the black hole (BH) singularity, namely

$$\Phi = 1 + \frac{m_1}{|r - r_1|} + \frac{m_2}{|r - r_2|} + u \quad (4)$$

with $r_{1,2}$ the locations of the BHs and u a regular function. The parameters $m_{1,2}$ are commonly referred as the *bare* or *puncture* masses. Ansorg [5] developed an elegant solver for Eq. (1) based on spectral methods called **2Punctures**. The solver is one of the most widely used codes by the numerical relativity (NR) community.

To construct astrophysically relevant BBH initial data, one thus needs to provide the values for the parameters $m_{1,2}$, $r_{1,2}$, $P_{1,2}^i$ and $S_{1,2}^i$. The most common approach for this is with the assistance of post-Newtonian (PN) approximations. PN equations of motion are used to evolve the BBH of interest from large separations until the separation at which the NR evolution will start. The parameters of the BBH at the end of the PN evolution are used as input parameters to solve Eq. (1). There is a subtlety here. The bare puncture masses $m_{1,2}$ are not the masses of the BHs. As first guess for these parameters, one uses the PN BH masses, but iterations are needed to adjust the puncture bare masses until the masses of the BHs match the desired PN masses.

There is an issue with the puncture BBH initial data as just described. For sufficiently large binary separations, one would expect the space-time in the neighborhood of each BH to be close to a boosted Kerr solution, or boosted Schwarzschild solution if the BH is not spinning. This is not the case for the puncture data with Bowen-York extrinsic curvatures, not even for a single BH. The reason for this are the conformal flatness assumption and the Bowen-York extrinsic curvatures. The space-time of a boosted or a Kerr BH is not conformally flat. Also, the Bowen-York extrinsic curvatures are not the extrinsic curvatures for a boosted or Kerr BH. As a

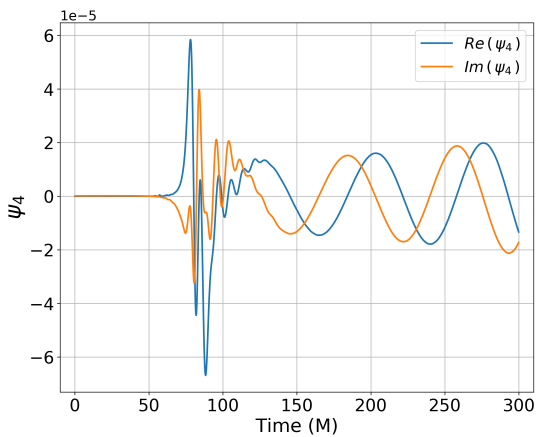


FIG. 1. The real and imaginary parts of the $l = 2$, $m = 2$ modes of Weyl scalar Ψ_4 extracted at a radius $75M$ for the waveform GT0860 in the Georgia Tech catalogue. This is an equal mass, precessing BBH system with spin magnitude of $a=0.8$. The junk radiation is evident at the beginning and appears to end around a time $134M$, with M the total mass of the binary.

consequence, the puncture Bowen-York initial data contain spurious or *junk* radiation.

In numerical evolutions, junk radiation manifests itself as a burst. Figure 1 depicts an example in terms of the Weyl scalar Ψ_4 as a function of time for the $l = 2$, $m = 2$ mode. There is an ongoing debate in the NR community about the extent to which the junk radiation introduces appreciable changes to the binary, specifically changes to the spins and masses of the BHs, and thus to the orbital dynamics of the binary [6–14]. Some of the studies attempt to tame the junk radiation by moving away from conformal flatness [7, 8], others introduce explicitly PN corrections [10]. Our view here is to obtain first a detailed characterization of the effects from junk radiation on the holes and then introduce adjustments in the input parameters of the binary that anticipates the changes produced by the junk radiation. The expectation is that, after the junk radiation dissipates away, one is left with the BBH system one originally intends to have.

Waveform Analysis: Our work is based on the Georgia Tech catalogue of BBH simulations [15]. The first step we took was to monitor in our simulations the behavior of the masses and spins of the BHs in a window between the initial time of the simulation and the end of the burst of junk radiation. Figure 2 shows the percent change δM_i in the initial irreducible mass of the BHs as a function of time for three binary simulations from the catalogue: GT0406, GT0407 and GT0866. The irreducible mass M_i is computed from the area A of BH horizon: $M_i = \sqrt{A/4\pi}$. It is evident in Fig. 2 the increase in the masses of the BHs during the first $20M$ of the simulation. This trend was observed in all the simulations for which we tracked the masses of the holes. Similar jumps were also

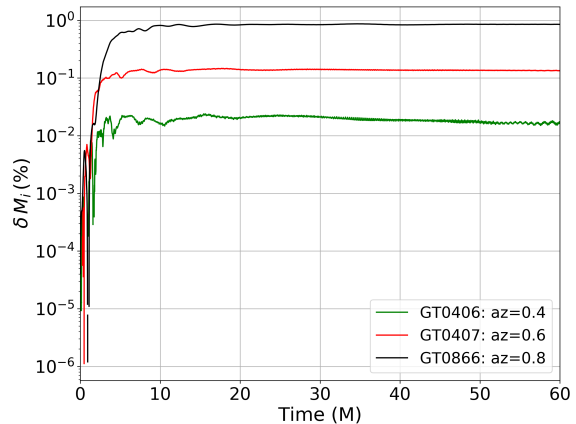


FIG. 2. The percent change in initial irreducible mass of the BHs for three simulations from the Georgia Tech catalogue: GT0406, GT0407 and GT0866. An increase in the mass is seen over a period of approximately $20M$.

observed in the spins.

Learning from single black hole simulations: Next we investigated whether the jumps in mass and spin were due to *local* effects in the neighborhood of the BHs or if they involved correlations between the holes in the binaries. To answer this question, we looked at the effects of junk radiation on a single BH. We carried out simulations expanding the dimensionless spin parameter $a = S/M_h^2$ in the range $0 \leq a \leq 0.8$ and the speed $v = P/M_h$ in the range $0 \leq v \leq 0.3$, with S the angular momentum, P linear momentum, and M_h the mass of the BH, where $M_h^2 = M_i^2 + S^2/(2M_i)^2$. The spin of the BH was aligned with the z -direction and the momentum with the y -direction. To a good approximation, these configurations cover the initial setups of BHs in the non-precessing BBH simulations in our catalogue.

Not surprisingly, the single BH simulations also showed increases in mass and spin. Furthermore, those increases took place, as with the BBH simulations, during the first $20M$ of the simulation time. This suggests that the effects of junk radiation are localized near the hole and do not depend on the presence of the other hole.

Figure 3 shows with points the percentage change in the BH irreducible mass δM_i and δa for all the single BH simulations as a function of the dimensionless spin a and speed v . The grey surfaces in Figure 3 are fits to the data where we use the following fitting function:

$$\begin{aligned}
 F = & c_{00} + c_{10}a + c_{20}a^2 + c_{30}a^3 + c_{40}a^4 + c_{50}a^5 \\
 & + c_{01}v + c_{02}v^2 + c_{03}v^3 + c_{04}v^4 + c_{05}v^5 \\
 & + c_{11}av + c_{12}av^2 + c_{13}av^3 + c_{14}av^4 \\
 & + c_{21}a^2v + c_{31}a^3v + c_{41}a^4v \\
 & + c_{22}a^2v^2 + c_{23}a^2v^3 + c_{32}a^3v^2
 \end{aligned} \tag{5}$$

The coefficients for the fit to δM_i and δa are given in Table I.

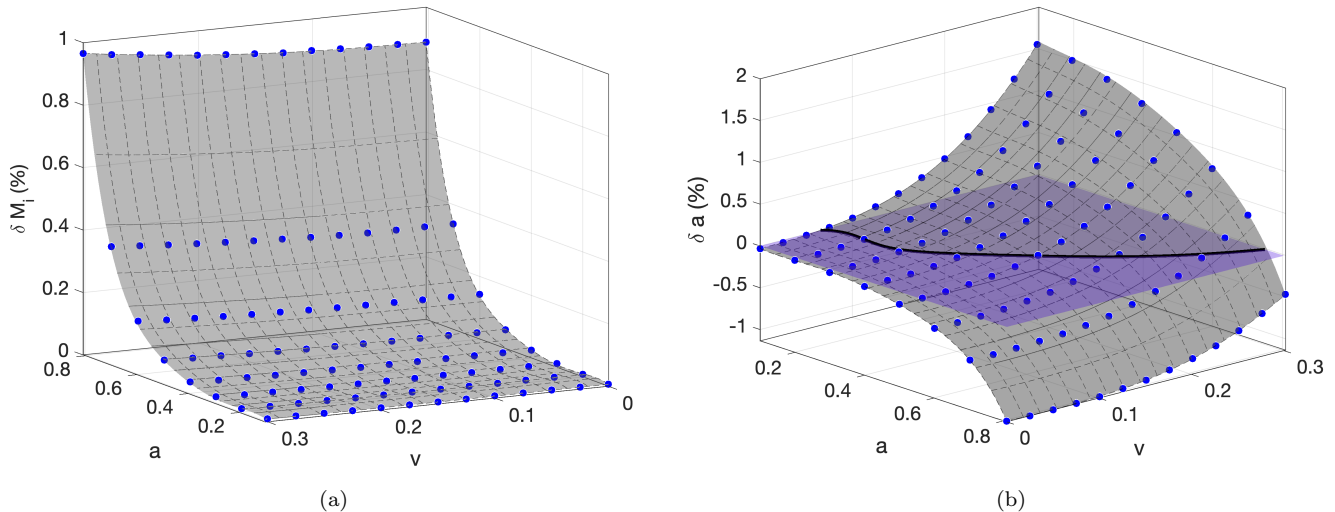


FIG. 3. Percent change in the (a) irreducible mass of the BH M_i and (b) dimensionless spin a in the single BH simulations as a function of a and v (blue dots). Two-parameter fits to the data by Eq. (5) are shown as a grey surfaces.

c_{ij}	δM_i	δa	c_{ij}	δM_i	δa
c_{00}	-0.09935	0.1294	c_{40}	-65.83	79.59
c_{10}	2.148	-3.169	c_{31}	-4.27	13.47
c_{01}	0.05612	-0.0977	c_{22}	-1.565	-5.56
c_{20}	-14.92	21.01	c_{13}	3.918	-13.17
c_{11}	-0.4674	1.118	c_{04}	-21.74	288.9
c_{02}	-0.6845	7.696	c_{50}	36.64	-40.72
c_{30}	46.3	-61.24	c_{41}	2.524	-7.763
c_{21}	2.386	-7.675	c_{32}	2.931	2.056
c_{12}	-0.2141	2.781	c_{23}	-0.7278	-35.24
c_{03}	5.791	-15.01	c_{14}	-5.623	12.7
			c_{05}	29.78	-413.8

TABLE I. Fitting coefficients for δM_i and δa in Eq. 5.

Interestingly, from Fig. 3a, the effect of junk radiation on the mass correlates stronger with the initial spin than with the speed of the puncture. This is not the case with the effect on the spin of the BH. As it can be seen from Fig. 3b, the junk radiation reduces the spin for larger initial spin and increases the spin for larger speeds. As a consequence, there is a family of cases for which the effects cancel out. These are the cases when the surface in Fig. 3b intersects the $\delta a = 0$ plane, and they are denoted with the black line. Another important finding was that the junk radiation only affected the magnitude of the spin but not its direction.

Connecting with binary black holes simulations: Once we quantified the changes in mass and spin for the single BH simulations, the next step was to investigate whether these changes are the same as those observed in each of the holes in BBH simulations. We looked at 107 bi-

nary simulations in our catalogue: 67 precessing binaries, and 40 aligned spin, non-precessing binaries. Figures 4a and 4b show with points δM_i and δa for the BHs in the BBHs (red for aligned spins and green points for precessing binaries). Grey surfaces denote the single BH fit. Figures 4c and 4d show the corresponding residuals. The residuals in the masses are $O(10^{-2})\%$, and for $v \lesssim 0.24$ the spin residuals are $O(10^{-1})\%$. On the other hand, for $v \gtrsim 0.24$ the spin residuals are $O(1)\%$ and all negative. Since the residuals are data-fit, this implies that the single BH fit overestimates the effect of junk radiation for $v \gtrsim 0.24$. For reference, BHs with $v \approx 0.24$ involve binary systems with initial separations of $\approx 10 M$ and gravitational wave frequency $\omega M \approx 0.048$. The levels of residuals for δM_i and for δa if $v \lesssim 0.24$ give us confidence that the fitting formula derived from single BH simulations provides good estimates applicable to binary simulations.

When to worry about junk radiation: Finally, we present a couple of examples of how the single BH junk radiation fits can be used in BBH simulations. From the waveforms in these simulations, we quantify whether one needs to worry about the effects of junk radiation in gravitational wave analysis for LIGO and LISA sources.

Assuming that one wants to simulate a binary with BHs having irreducible masses $M_i^{1,2}$, spins $a^{1,2}$ and speeds $v^{1,2}$, the task is to find irreducible masses $\bar{M}_i^{1,2}$ and spins $\bar{a}^{1,2}$ to use in the initial data such that the junk radiation modifies these values and yields the desired values $M_i^{1,2}$ and $a^{1,2}$. The adjusted values $\bar{M}_i^{1,2}$ and $\bar{a}^{1,2}$ can be found by solving the following equations:

$$M_i^{1,2} = [1 + \delta \bar{M}_i^{1,2}(\bar{a}^{1,2}, v^{1,2})] \bar{M}_i^{1,2} \quad (6)$$

$$a^{1,2} = [1 + \delta \bar{a}^{1,2}(\bar{a}^{1,2}, v^{1,2})] \bar{a}^{1,2} \quad (7)$$

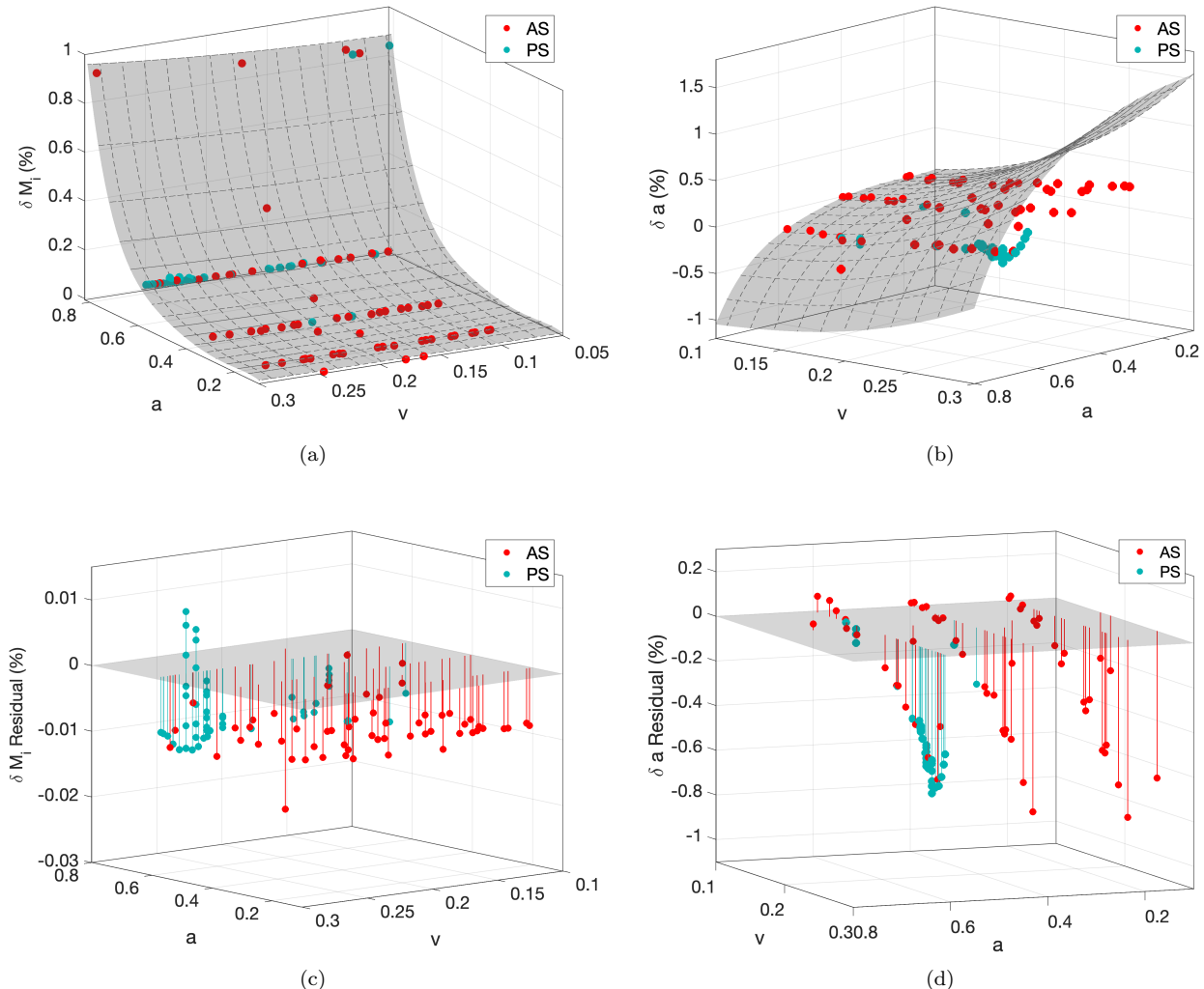


FIG. 4. A comparison between the percent changes (a) δM_i and (b) δa in BH irreducible masses in BBH simulations (red for aligned spins and green for precessing binaries) with the single BH fit (grey surface). Residuals := (data - fit) between the single BH fit and the BBH data are shown in (c) and (d).

where the junk radiation changes in the formulas above are given as fractional changes not percentages. As mentioned before, for BHs moving with speeds $\gtrsim 0.24$, the formulas overestimate the correction on the spin magnitude. For those cases, we estimate that only a 10% correction should be applied.

Figure 5 depicts the $l = 2$, $m = 2$ mode of Weyl scalar Ψ_4 for two pairs of simulations. All four simulations consist of equal mass, aligned spin binaries. The top panel shows the cases with $a \approx 0.6$ and the bottom for $a \approx 0.8$. In blue is the waveform from the *raw* simulation and in orange the waveform in which the masses and spins have been adjusted according to the single BH fitting formulas. The mass of the BH, its irreducible mass and spin magnitude at the beginning of the simulation and after the junk radiation has dissipated

Type	$t = 0$			$t > t_{\text{junk}}$		
	M_h/M	M_i/M	a	M_h/M	M_i/M	a
raw	0.4994	0.4736	0.6013	0.5004	0.4744	0.6032
adj	0.4985	0.4729	0.6000	0.4994	0.4736	0.6018
raw	0.4972	0.4430	0.8090	0.5001	0.4471	0.8013
adj	0.4939	0.4387	0.8161	0.4971	0.4431	0.8079

TABLE II. Mass of the BH, its irreducible mass and spin magnitude at the beginning of the simulation and after the junk radiation has dissipated.

are given in Table II. Notice that with the junk adjustment $M_i/M(t > t_{\text{junk}}; \text{adj}) \approx M_i/M(t = 0; \text{raw})$ and $a(t > t_{\text{junk}}; \text{adj}) \approx a(t = 0; \text{raw})$, as needed.

The mismatches ϵ between the waveform from *raw* and adjusted simulations in Advanced LIGO are shown in

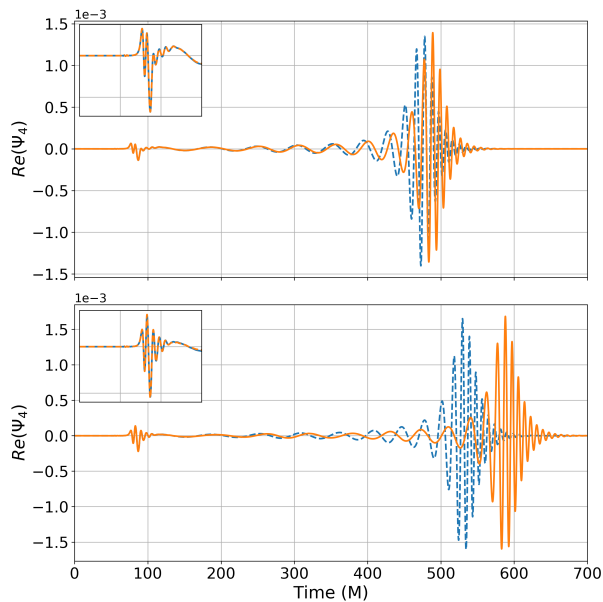


FIG. 5. Mode (2,2) of Ψ_4 for two equal mass, aligned spin binaries. Top panel shows the cases with $a \approx 0.6$ and the bottom for $a \approx 0.8$. In blue is the waveform from the *raw* simulation and in orange the waveform in which the masses and spins have been adjusted according to the single BH fitting formulas. Insets focus on the junk radiation.

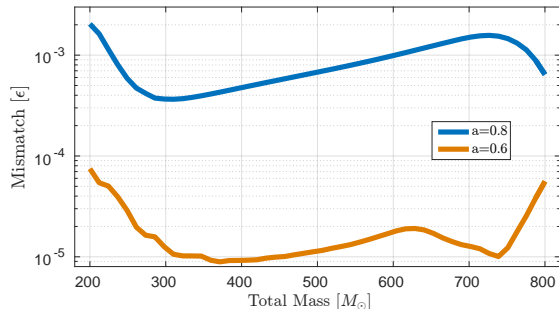


FIG. 6. Mismatch as a function of total-mass of the binary for waveforms from the *raw* and adjusted with masses and spins. The blue cover refers $a \approx 0.6$ and the yellow is for $a \approx 0.8$. The mismatch has been computed for Advanced LIGO design noise and masses are kept in the detector frame.

Figure 6. For $a \approx 0.8$, $\epsilon \sim 10^{-3}$ in average, while for $a \approx 0.6$, $\epsilon \sim 10^{-5}$. To avoid astrophysical inference with a bias, one needs $\epsilon \rho^2 \lesssim 1$ [16]. This implies that waveforms of sources with highly spinning BH measured with S/N of $\rho \gtrsim 30$ will exhibit inference biases if they are not corrected for the junk radiation. For future detectors such as the Einstein Telescope and LISA, even low spin sources with $\rho \gtrsim 10^2$ would require junk radiation correction.

Conclusion: Using simulations of single punctures with different spins and linear momentum, we have investi-

gated the effect of junk radiation on the mass and spin of the BH. We found that junk radiation does not affect the direction of the spin. With these results, we obtained fitting functions that can be used to predict changes in the masses and spin magnitudes of BHs in binary systems. We tested the effectiveness of the fitting functions and showed that for binary systems with highly spinning BHs, inference biases would be introduced by waveforms that not are corrected for junk radiation in sources with SNRs $\gtrsim 30$.

Acknowledgements: Work supported by NSF grants 1806580, 1809572, 1550461, and XSEDE allocation TG-PHY120016.

-
- [1] T. W. Baumgarte and S. L. Shapiro, *Numerical Relativity: Solving Einstein's Equations on the Computer* by Thomas W. Baumgarte and Stuart L. Shapiro. Cambridge University Press, 2010. ISBN: 9780521514071 (Cambridge University Press, 2010).
 - [2] L. L. Smarr, ed., *Sources of Gravitational Radiation* (1979).
 - [3] J. M. Bowen and J. W. York, Jr., Phys. Rev. D **21**, 2047 (1980).
 - [4] S. Brandt and B. Bruegmann, Phys. Rev. Lett. **78**, 3606 (1997), arXiv:gr-qc/9703066 [gr-qc].
 - [5] M. Ansorg, B. Bruegmann, and W. Tichy, Phys. Rev. **D70**, 064011 (2004), arXiv:gr-qc/0404056 [gr-qc] CITATION = GR-QC/0404056; .
 - [6] M. Hannam, S. Husa, B. Brügmann, J. A. González, and U. Sperhake, Classical and Quantum Gravity **24**, S15 (2007), arXiv:gr-qc/0612001 [gr-qc].
 - [7] G. Lovelace, Classical and Quantum Gravity **26**, 114002 (2009), arXiv:0812.3132 [gr-qc].
 - [8] N. K. Johnson-McDaniel, N. Yunes, W. Tichy, and B. J. Owen, Phys. Rev. D **80**, 124039 (2009), arXiv:0907.0891 [gr-qc].
 - [9] T. Chu, H. P. Pfeiffer, and M. A. Scheel, Phys. Rev. D **80**, 124051 (2009), arXiv:0909.1313 [gr-qc].
 - [10] B. J. Kelly, W. Tichy, Y. Zlochower, M. Campanelli, and B. Whiting, Classical and Quantum Gravity **27**, 114005 (2010), arXiv:0912.5311 [gr-qc].
 - [11] F. Zhang and B. Szilágyi, Phys. Rev. D **88**, 084033 (2013), arXiv:1309.1141 [gr-qc].
 - [12] K. Slinker, C. R. Evans, and M. Hannam, Phys. Rev. D **98**, 044014 (2018), arXiv:1806.08364 [gr-qc].
 - [13] I. Ruchlin, *Puncture Initial Data and Evolution of Black Hole Binaries with High Speed and High Spin*, Ph.D. thesis, Rochester Institute of Technology (2015).
 - [14] U. Sperhake, V. Cardoso, C. D. Ott, E. Schnetter, and H. Witek, Phys. Rev. D **84**, 084038 (2011), arXiv:1105.5391 [gr-qc].
 - [15] K. Jani, J. Healy, J. A. Clark, L. London, P. Laguna, and D. Shoemaker, Class. Quant. Grav. **33**, 204001 (2016), arXiv:1605.03204 [gr-qc] CITATION = ARXIV:1605.03204; .
 - [16] L. Lindblom, B. J. Owen, and D. A. Brown, Phys. Rev. D **78**, 124020 (2008), arXiv:0809.3844 [gr-qc].